Identification of very long-chain (>C_{24}) fatty acid methyl esters using gas chromatography coupled to quadrupole/time-of-flight mass spectrometry with atmospheric pressure chemical ionization source

B. Garlito [a], T. Portolés [a*], W.M.A Niessen [b], J. C. Navarro [c,d], F. Hontoria [c,d], Ó. Monroig [e], I. Varó [c,d] and R. Serrano [a,d]

[(a)] Research Institute for Pesticides and Water (IUPA), University Jaume I, Av. Sos Baynat S/N, 12071, Castellón, Spain

[(b)] hyphen MassSpec, Margrietstraat 34, 2215 HJ Voorhout, The Netherlands

[(c)] Instituto de Acuicultura Torre de la Sal (IATS-CSIC), Ribera de Cabanes, S/N, 12595, Cabanes, Castellón, Spain

[(d)] Associated Unit of Marine Ecotoxicology (IATS-IUPA), Ribera de Cabanes, S/N, 12595, Cabanes, Castellón, Spain

[(e)] Institute of Aquaculture, Faculty of Natural Sciences, University of Stirling, Stirling FK9 4LA, Scotland, UK

[*]Corresponding author: tportole@uji.es. Phone: +34 964387339

ABSTRACT

Gas chromatography coupled to a quadrupole time-of-flight mass analyzer (QTOF) with an atmospheric pressure chemical ionization (APCI) source has been tested to study the ionization and mass spectrometric behavior of long-chain and very long-chain polyunsaturated fatty acids (LC-PUFAs, $C_{18–24}$; VLC-PUFAs, $>C_{24}$). The protonated molecule ($[M+H]^+$), measured at accurate mass, became the base peak of the spectrum for all the studied compounds and was promoted by the addition of water into the source. This fact overcame the existing difficulties for the identification of VLC-PUFAs when using an electron ionization source (EI). The extensive fragmentation of PUFAs in this source is the main drawback due to the fact that since reference standards are not commercially available, final identification relies on retention time estimation. The application of GC–APCI-QTOF to the screening of lipid extracts from the eyes of different fish species added confidence to the identification of several VLC-PUFAs. Further investigation of ion ratios allowed to predict the position of key double bonds enabling the classification of VLC-PUFAs as ω3 or ω6 compounds. VLC-PUFAs spectra found in biological samples were compared to those obtained from corresponding peaks found in heterologous expression experiments of fish's Elovl4.

Keywords: gas chromatography; quadrupole time-of-flight mass spectrometry; atmospheric pressure chemical ionization source; very long-chain polyunsaturated fatty acids

1. INTRODUCTION

Fatty acids (FAs), besides being a source of energy, are essential compounds involved in different physiological and metabolic processes, like cell membrane formation or signal transduction, that ensure the correct cellular functioning [1]. Among FAs, certain long-chain (C_{18-24}) polyunsaturated fatty acids (LC-PUFAs) including arachidonic acid (20:4ω6), eicosapentaenoic acid (20:5ω3) and docosahexaenoic acid (22:6ω3) play pivotal roles in inflammatory response and function and in development of the central nervous system [2]. Several studies have demonstrated the influence of LC-PUFAs in neural development, neurodegenerative diseases, and visual system in mammals [3,4].

Besides, the very long-chain (>C_{24}) polyunsaturated fatty acids (VLC-PUFAs), biosynthesized in vertebrates by FA elongase enzymes such as Elovl4 [5], have been regarded as essential for cognitive development, retinal function and reproductive processes [6–10]. Consequently, VLC-PUFAs are typically found in low concentrations in specific lipid classes such as phosphatidylcholine (PC), sphingomyelin and ceramides in brain, retina and gonads of vertebrates [11], and their importance has been related to their structure combining a proximal carboxylic region similar to saturated FAs and a distal region with PUFA character [8]. In addition to being present in specific lipid classes from certain tissues in very small amounts compared to their shorter chain counterparts, the lack of standards and references in mass spectrometry libraries have involved an analytical challenge for their determination and characterization.

Liquid and gas chromatography (LC and GC) coupled to mass spectrometry (MS) have been the techniques chosen to carry out both quantitative and qualitative analysis. On the one hand, LC-MS techniques based on electrospray ionization (ESI) or atmospheric pressure chemical ionization (APCI) have been commonly applied for the analysis of lipid

species containing VLC PUFAs [8]. To achieve this, LC in normal and reversed phase are used but long chromatographic runs are required to achieve good chromatographic separation between polar species [12,13]. In order to facilitate the quantitative analysis of total VLC-PUFAs, hydrolysis must be performed leading to LC-ESI-MS in negative-ion mode the required technique. However, the drawbacks of low specificity in the negative-ion MS detection mode and requirement of the post-column addition of a cationizating agent after acidic chromatographic separation have hindered a simple way of FA analysis. Thus, derivatization of FA must be finally applied to facilitate their analysis by LC-ESI-MS in positive-ion mode [14].

On the other hand, while a derivatization step is also required, GC is the most frequently used technique in this field. To improve the separation performance, comprehensive two dimensional gas chromatography (GC×GC) has also been applied to clarify the identity of fatty acid isomers [15]. Although selective GC stationary phases like polyethylene glycols or cyanopropyl silicones (medium-high polarity) are widely applied for the analysis of FAMEs (C < 24), for the study of VLC-PUFA 5%-(phenyl)-methylpolysiloxane columns are more convenient as the applicable upper temperature limit (350ºC) is higher than the selective ones (260ºC). Under these conditions, VLC-PUFA (C > 24) can be analyzed avoiding column degradation. GC-MS with electron ionization (EI) is frequently applied for the analysis of VLC-PUFAs [16] since it provides complete information about the fragmentation patterns of FA derivatives. Among others, methyl esters (FAMEs) are commonly used in FA analysis [17]. However, the extensive fragmentation of FAMEs in EI source involves the partial or total loss of the highly diagnostic molecular ion ($M^{+\bullet}$) and generates the same EI spectra for unsaturated FAMEs (ω6 or ω3) with different chain length [18]. This fact, together with the absence of reference standards, hinders the identification process of VLC-PUFAs. In this context,

APCI combined with GC-MS instruments has revealed as a useful alternative to EI. As it has been demonstrated in several fields [19–24], the soft and universal ionization in this source provides abundant $M^{+\bullet}$ and/or $[M+H]^+$ in the mass spectra, thus substantially improving the identification capability, as well as enhancing sensitivity and selectivity for the detection of analytes in the samples [25,26]. Under these circumstances, the use of GC-APCI-QTOF MS will add confidence to the identification of VLC-PUFA.

Since their detection in bovine retinas by Aveldaño et al. in 1987 [27], the study of VLC-PUFAs has been mainly focused on mammals [9,11,12,28,29]. However, the detection and characterization of these compounds in fish has been scantily studied despite being the main source of ω3 LC-PUFAs in human's diet [30]. Studies in fish have focused on elucidating the molecular mechanisms underlying the biosynthesis of VLC-PUFAs, particularly the roles that elongase enzymes such as Elovl4 play in these metabolic pathways [2,31].

The aim of this work is the development of a reliable analytical methodology for detection and identification of VLC-PUFAs, for which no commercially available standards exist, in the PC fraction of lipid extracts from the eyes of different fish species. The potential of GC-APCI-QTOF MS to provide accurate mass measurement of intact $M^{+\bullet}$ and/or $[M+H]^+$, was considered to add confidence in the identification step. For this purpose, a range of commercially available saturated and polyunsaturated LC-PUFA methyl esters were analyzed by GC-APCI-QTOF MS and their ionization and fragmentation behavior was studied. Additionally, relationships between the fragmentation patterns and FAME structures have been studied in order to differentiate ω3 from ω6 VLC-PUFAs' series without the need of reference standards. As a final step, in order to confirm the identity of detected compounds, heterologous expression experiments were carried out. To the

best of our knowledge, GC-APCI-QTOF MS has not been applied for the determination of VLC-PUFA methyl esters yet.

2. EXPERIMENTAL

2.1 Standard compounds, solvents and reagents

Methyl stearate (18:0-ME), methyl arachidate (20:0-ME), methyl behenate (22:0-ME) and methyl tetracosanoate (24:0-ME) standards were purchased from Fluka (Zwijndrecht, The Netherlands). Methyl hexacosanoate (26:0-ME), methyl octacosanoate (28:0-ME) and methyl triacontanoate (30:0-ME) standards were purchased from Dr. Ehrenstorfer (Augsburg, Germany). Arachidonic acid methyl ester (20:4ω6-ME), cis-5,8,11,14,17-eicosapentaenoic acid methyl ester (20:5ω3-ME), cis-7,10,13,16-docosatetraenoic acid methyl ester (22:4ω6-ME), cis-7,10,13,16,19-docosapentaenoic acid methyl ester (22:5ω3-ME), cis-4,7,10,13,16,19-docosahexaenoic acid methyl ester (22:6ω3-ME), 20:4ω3-ME, 22:4ω3-ME, and 24:5ω3 standards were purchased from Supelco (Bellefonte, PA, USA).

Stock solutions (around 500 μg mL^{-1} and 1 μg mL^{-1} for 24:0-ME and 26:0-ME) were prepared by dissolving solid reference standards in hexane or by diluting reference standard solutions in hexane and subsequently stored in a freezer at -20 ºC under a N_2 atmosphere. Working solutions were prepared by diluting stock solutions in hexane.

Hexane (ultra-trace quality) was purchased from Scharlab (Barcelona, Spain). Chloroform ($CHCl_3$), diethyl ether and toluene were purchased from Merck Millipore (Darmstadt, Germany). Methanol (MeOH) was purchased from VWR (Radnor, PA, USA). Sulfuric acid, glacial acetic acid and potassium chloride (KCl) were purchased from Panreac (Castellar del Vallés, Barcelona, Spain). Iodine and butylated hydroxytoluene (BHT, content >99%), used as antioxidant, were purchased from Sigma

Aldrich (St. Louis, MO, USA). All reagents were analytical grade. HPLC-grade water was obtained by purifying double distilled water in a Milli-Q Gradient A10 system (Millipore, Bedford, MA, USA).

2.2 Samples

Fish eyes

Twelve eyes from adult specimens of fish species including the European seabass (2), gilthead seabream (1), Atlantic salmon (1) and Senegalese sole (8) were dissected and cleaned from other tissues. Next, the crystalline lens was removed and stored at -20 ºC for further treatment.

Elongated fatty acids by Elovl4 protein

Further biological samples containing VLC-PUFAs were generated by expressing the coding region of the Atlantic salmon Elovl4 in yeast *Saccharomyces cerevisiae* which was grown in the presence of one of the following polyunsaturated fatty acid (PUFA) substrates: 20:4ω3, 22:4ω6, 22:5ω3, 22:6ω3, 24:5ω3. A previous study confirmed that the Atlantic salmon Elovl4 could efficiently elongate some of these PUFA substrates to produce polyenes up to 36 carbons [32]. After 48 h, yeast samples were harvested and washed twice with double distilled water and kept at -20 ºC until further treatment [32]. Given that Elovl4 enzymes add 2-carbon units to FA substrates [33], all these PUFA substrates provided a set of step-wise elongation products that could be easily identified in the chromatogram since both FA substrates and products are absent in yeast.

2.3 Sample treatment

Total lipids were extracted according to the method of Folch et al. [34]. Briefly, samples (fish eyes and yeast) were homogenized in $CHCl_3$:MeOH (2:1, v/v) with BHT (0.01%, w/v). After addition of 0.25 % (v:v) aqueous solution of KCl (0.88%, w/v), the lower organic phase was filtered (70 μm Whatman filter paper), evaporated to dryness under a stream of nitrogen and kept in desiccator overnight. The extracts were then weighed to determine the total amount of lipids, redissolved in $CHCl_3$:MeOH (2:1) (10 mg/ml) and stored at -20 °C.

Phospholipid classes were separated following the method developed by Olsen et al. [35] consisting in 20 cm × 20 cm TLC plates (Silica gel G 60 (Merck, Darmstadt, Germany) run in a polar solvent system of methyl acetate:isopropanol:$CHCl_3$:MeOH:0.25% (w/v) KCl (25:25:25:10:9 by volume). A well known Artemia nauplii extract [36] run in parallel to the samples allowed the location of the PC fraction on the plates after using a 1% (w/v) iodine solution in $CHCl_3$ for lipid dying. PC spots were scrapped off and submitted to acid-catalyzed transesterification [37]. Resulting fatty acid methyl esters (FAMEs) were stored at -20 °C in hexane/BHT (0.01%) under nitrogen, until chromatographic analysis.

2.4 Instrumental

GC–APCI-(Q)TOF MS

An Agilent 7890 N gas chromatograph (Palo Alto, CA, USA) equipped with an Agilent 7683 autosampler was coupled to a quadrupole orthogonal acceleration time-of-flight mass spectrometer, Xevo G2 QTOF (Waters Corporation, Manchester, UK), operated in APCI mode. A fused silica HP-5MS capillary column with a length of 30 m × 0.25 mm i.d. and a film thickness of 0.25 μm with a 1 m × 0.25 mm i.d. deactivated post-column (J&W Scientific, Folson, CA, USA) was used for GC separation. The oven temperature was programmed as follows: 60 ºC (1 min); 40 ºC/min to 180ºC; 10 ºC/min to 320 ºC (4

min). Pulsed splitless (30 psi) injections of 1 μL were carried out at 280 ºC with a splitless time of 1 min. Helium 99.999% (Praxair, Spain) was used as carrier gas at a flow of 2 mL min^{-1}.

The interface and ionization source temperatures were set to 320 ºC and 150 ºC, respectively. N_2 was used as auxiliary gas at 175 L h^{-1}, as cone gas at 25 L h^{-1} and as make-up gas at 300 mL min^{-1}. The APCI corona discharge pin was operated at 1.2 μA and the cone voltage was set to 20 V.

The QTOF was operated at 2.5 spectra s^{-1} acquiring the mass range *m/z* 50–650. The TOF MS resolution was approximately 15,000 (FWHM) at *m/z* 264. Acquisition was done in MS^E mode in which two alternating acquisition functions with different collision energies were generated: the low-energy (LE) function, selecting a collision energy of 4 eV to avoid or minimize fragmentation, and the high-energy (HE) function, with a collision energy ramp ranging from 25 to 40 eV to obtain a greater range of fragment ions.

Perfluorotributylamine (Sigma Aldrich, Madrid, Spain) was used for the daily mass calibration. Internal calibration was performed using a background ion from the GC-column bleed as lock mass (protonated molecule of hexamethylcyclotrisiloxane, *m/z* 223.0642).

In order to work under proton transfer conditions, an uncapped vial containing water was placed in a designed holder into the APCI source door to enhance protonation. MS data were acquired in centroid mode and processed by the ChromaLynx XS application manager (within MassLynx v4.1; Waters). Mass-Fragment software (Waters) was used for mass spectra interpretation.

3. RESULTS AND DISCUSSION

3.1 Ionization behavior of FAMEs

The ionization behavior was tested using all commercially available FAME standards with a focus on their differences in the degree of unsaturation and position of the last double bond: saturated (18:0-ME, 20:0-ME, 22:0-ME,24:0-ME, 26:0-ME, 28:0-ME and 30:0-ME) and unsaturated (20:4ω3-ME, 20:4ω6, 20:5ω3-ME, 22:4ω3-ME, 22:4ω6, 22:5ω3-ME, 22:6ω3-ME, and 24:5ω3-ME). As it has been described in previous studies, two ionization mechanisms can take place simultaneously in the APCI source: charge transfer promoting the formation of $M^{+\bullet}$ and/or protonation [38]. In many cases, protonation is directly produced by the water traces present in the N_2 supply. However, it can be enhanced using protic solvents as modifier [20]. Some experiments regarding analyte ionization were made in order to evaluate the effect of the addition of modifiers in the source.

Despite no protic modifier was initially added into the source, the protonated molecule $[M+H]^+$ was the base peak in the spectrum for all analytes. For saturated FAMEs, the molecular ion $M^{+\bullet}$ was also formed from 39 to 86%, showing a higher tendency of protonation when the number of carbon atoms decreased (see **Figure 1a up**). In the case of ω3 and ω6 FAMEs, $M^{+\bullet}$ was generated from 40 to 75% and 23 to 71%, respectively, showing a higher tendency of protonation when the number of carbon atoms decreased and the unsaturation degree increased (see **Figure 1b-c up**)

Taking into account the proneness of FAMEs to protonation, a subsequent experiment using water as modifier in the source was carried out. In this way, the proton transfer mechanism was enhanced, decreasing the relative abundance of $M^{+\bullet}$ (**Figure 1 down**). $M^{+\bullet}$ still appeared in the spectra, but only in a percentage among 7-10% for saturated FAMEs (with the same protonation tendency as for charge transfer conditions), 8-12% for ω6 and 7-9% for ω3 FAMEs showing higher protonation affinity of the smallest FAMEs with highest degree of unsaturation. Therefore, because of both the better

sensitivity of protonated molecule and higher spectral purity, it was decided to use water as modifier for further experiments.

As a consequence of the soft ionization character of the APCI source, low in-source fragmentation of FAMEs was observed if compared with their corresponding EI spectra taken from NIST library. As it has been reported in other studies, EI spectra of saturated FAMEs are dominated by the ion with *m/z* 74 $[CH_2C(OH)OCH_3]^{+\bullet}$ resulting from a McLafferty rearrangement (**Figure 2a**), whereas the ion with *m/z* 79 $[C_6H_7]^+$ is usually the base peak in mass spectra of FAMEs with three or more methylene-interrupted double bonds (**Figure 2c**) [17]. Exploring the APCI spectra of saturated FAMEs, no in-source fragment ions were observed. Thus, $[M+H]^+$ is completely preserved (**Figure 2b**). Regarding polyunsaturated ω6 and ω3 FAMEs, all of them exhibited $[M+H-CH_3OH]^+$ in-source fragments with relative abundances between 4-11% and 2-6%, respectively. In addition, less abundant $[M+H-CH_3OH-H_2O]^+$ fragments were also found for all polyunsaturated FAMEs (**Figure 2d**).

3.2 Fragmentation behavior of FAMEs

FAMEs share a common methyl ester group. The oxygen atoms are the only structural features with lone electron pairs, thus being the most feasible sites for protonation. Taking into account the proton affinity of the carbonyl and methyl ether groups, the expected protonation site would be the oxygen atom of the carbonyl function. However, the degree of unsaturation plays an important role in ionization/fragmentation behavior, as is described below.

3.2.1 Group I. Saturated FAMEs

All saturated FAMEs showed $[M+H]^+$ as the base peak of the spectrum at LE due to the protonation of the carbonyl function. At HE conditions, the spectra are characterized by the presence of the ion with *m/z* 103.0759 ($C_5H_{11}O_2^+$) as the base peak, with a subsequent neutral loss of HCOOH producing the fragment ion with *m/z* 57.0704 ($C_4H_9^+$). For this class of compounds, although being unusual, apparently charge-remote fragmentation occurs and series of $C_{2n}H_{4n}$ losses from the hydrocarbon chain are observed.

3.2.2 Group II. ω6 and ω3 FAMEs

All ω6 and ω3 FAMEs showed a common fragmentation pathway showing fragment ions with the same *m/z*, irrespective the ω6 or ω3 character. After studying it at the HE function, none of the fragment ions by itself was specific for either the ω3 or the ω6, as in most cases only abundance differences seemed to be observed. This constitutes an inconvenience in the characterization of VLC-PUFAs for which no reference standards are (commercially) available. The presence of the $[M+H]^+$ in the LE spectrum together with the fragmentation information of the HE spectrum allows to tentatively identify the VLC-PUFA in terms of carbon chain length and the degree of unsaturation. At this point, it was considered to use of abundance ratios to distinguish between the ω6 and ω3 compounds. For that, all the spectral information available for the commercial reference standards was used to create a data matrix that contained the abundance for each *m/z* ion. Data were normalized to the ion with *m/z* 121 which was the base peak of spectrum from the 22:4ω3 and 22:4ω6. Inverse values were then calculated in order to work with values above 1. Among them, there were standards with different chain lengths (C_{20}-C_{24}) and different degrees of unsaturation (4, 5 and 6) for ω3 while only C_{20} and C_{22} with a degree of unsaturation of 4 were available for ω6.

Firstly, considering a completely unbiased analysis, a principal component analysis (PCA) was applied over the training data matrix. **Figure 3a** illustrates the PCA obtained in which a rough distinction between ω3 and ω6 can be appreciated. The next step consisted in performing an orthogonal partial least squares-discriminant analysis (OPLS-DA), which considers additional information about the two groups during classification. Thus, an OPLS-DA was applied to construct a statistical model that highlight differences in ion ratios between the two groups. As it can be seen, the OPLS-DA analysis separated the two groups of samples. For this purpose, an S-Plot graphic for ω3 vs ω6 was obtained (**Figure 3b**) and studied looking for endpoints. Theoretically, in an S-Plot the points with a p-corr value between 0.9 and 1 are closely related to the compounds characterizing the samples of one group, which constitute important class markers. According to this, only one marker (ion ratio for the ions with *m/z* 121 and 163) was selected. Returning to the data, we could observe that ω3 compounds used for the model construction presented ion ratios in the range of 4-10 while ω6 were found to be in the range of 17-24. Thus, this ion-ratio procedure was used for further experiments.

3.3 Analysis of adult fish eyes samples

The system (GC–APCI-QTOF MS in MS^E mode) was used for the eye extracts analysis. Data were processed using ChromaLynx XS software in combination with a homemade compound database that contained the elemental composition, retention time and fragments information previously obtained from the study with commercially available reference standards (C_{20}-C_{22}). Additionally, this database was extended with those FAMEs reported in the literature, mainly VLC-PUFAs for which reference standards were not commercially available (C_{24}-C_{34}), and whose reliable identification is considered an additional value given by GC–APCI-QTOF MS. The ChromaLynx XS application manager obtained eXtracted Ion Chromatograms (XICs) at LE and HE functions (0.02 Da window) for *m/z* values corresponding to the theoretical exact masses of the protonated molecules and the fragments (if known), respectively.

Table 1 summarizes the positive findings of FAMEs detected in the fish eye samples analyzed from the different species. Detection was initially based on the presence of $[M+H]^+$ in the LE function. Further investigation of fragment ions from the HE function together with the application of the ion-ratio procedure developed allowed their tentative identification. As an example, **Figure 4** illustrates the detection and tentative identification of 32:6ω3-ME in a gilthead sea bream eyes sample by GC–APCI-QTOF MS. The protonated molecule of 32:6-ME with *m/z* 483.4197 ($C_{33}H_{55}O_2^+$) was detected in the LE function with a mass error of 1.0 ppm. As the reference standard was not available, chemical structures for the most abundant fragment ions were suggested based on their accurate masses, using the Mass-Fragment software. All structures proposed for the fragments were compatible with the chemical structure of 32:6-ME making the identification even more reliable. At this point, the ion-ratio procedure developed was applied in order to decide whether it was ω3 or ω6. The ratio of *m/z* 121 and *m/z* 163 was

calculated to be a value of 4.6, which thus indicates to correspond to ω3, being 32:6ω3-ME.

3.4 Analysis of heterologous expression experiments and validation of the ion-ratio procedure

In order to confirm the identity of detected compounds and validate the developed ion-ratio procedure for the characterization of ω3 and ω6 VLC-PUFAs, heterologous expression experiments were carried out in order to establish retention times for VLC-PUFAs and compare the obtained spectra. As it has been explained in the introduction, Elovl4 proteins enable the elongation of PUFAs including, among others, 20:4ω6 (arachidonic acid), 20:5ω3 (eicosapentaenoic acid) and 22:6ω3 (docosahexaenoic acid) [2]. In order to expand our VLC-PUFA database, 20:4ω3, 22:4ω6, 22:5ω3, 22:6ω3 and 24:5ω3 FAs were individually used as elongation substrates for the Atlantic salmon Elovl4, a protein that had previously shown elongase capacity towards all these compounds [32]. **Figure 5** shows the XIC for the elongation products coming from 22:6ω3 (up) and 22:5ω3 (down). All the elongation products and substrates were evaluated and the information obtained allowed the final identification of the expected compounds.

4. CONCLUSIONS

The use of an APCI interface in GC–QTOF has been employed for the first time to study the ionization and fragmentation behavior of FAMEs. The addition of water in the source as modifier promoted the proton transfer reaction producing mainly $[M+H]^+$ species. In contrast to EI, low in-source fragmentation occurred in APCI. This fact together with the preservation of the protonated molecule measured at accurate mass has given an

additional value to the reliable identification of VLC-PUFAs in real samples. The ratio between the ions with *m/z* 121 and *m/z* 163 has been used for differentiation of ω3 and ω6 congeners. In addition, the heterologous expression experiments have enabled expanding our VLC-PUFA spectral library, and also establishing retention times for non-commercially available standards, thus improving characterization, identification and confirmation purposes. Results obtained in this paper will help to advance into the knowledge of the metabolism of these compounds.

FIGURE CAPTIONS

Figure 1. APCI spectra at the LE function of (a) Arachidic acid ME (saturated); (b) C22:6ω3-ME; and (c) C20:4ω6-ME under charge transfer (up) and protonation conditions (down).

Figure 2. Comparison of the in-source fragmentation for arachidic acid ME (up) and C20:5ω3-ME (down) in EI (left) and APCI (right) sources.

Figure 3. (a) PCA plot corresponding to the reference standards analyzed to create the model; (b) SPLOTs ω-3 versus ω-6.

Figure 4. Detection and identification of 32:6ω3-ME in a gilthead sea bream eyes sample by GC–QTOF MS (the reference standard was not available at our laboratory at the time of the detection): (a) Extracted-ion chromatograms (0.02 Da window) for protonated molecule in LE function and different fragment ions in HE function; (b) LE (bottom) and HE (top) spectra of the compound eluting at 18.6 min. Proposed elemental composition for fragment ions.

Figure 5. Extracted ion chromatograms for the elongation products coming from 22:6ω3 (up) and 22:5ω3 (down).

REFERENCES

[1] P.C. Calder, N-3 Fatty Acids, Inflammation and Immunity: New Mechanisms To Explain Old Actions., Proc. Nutr. Soc. 72 (2013) 326–36. doi:10.1017/S0029665113001031.

[2] O. Monroig, J. Rotllant, J.M. Cerdá-Reverter, J.R. Dick, A. Figueras, D.R. Tocher, Expression and role of Elovl4 elongases in biosynthesis of very long-chain fatty acids during zebrafish Danio rerio early embryonic development, Biochim. Biophys. Acta - Mol. Cell Biol. Lipids. 1801 (2010) 1145–1154. doi:10.1016/j.bbalip.2010.06.005.

[3] C.I.F. Janssen, A.J. Kiliaan, Long-chain polyunsaturated fatty acids (LCPUFA) from genesis to senescence: The influence of LCPUFA on neural development, aging, and neurodegeneration, Prog. Lipid Res. 53 (2014) 1–17. doi:10.1016/j.plipres.2013.10.002.

[4] E.J. Johnson, E.J. Schaefer, Potential role of dietary n-3 fatty acids in the prevention of dementia and macular degeneration., Am. J. Clin. Nutr. 83 (2006) 1494S–1498S.

[5] G. Schmitz, J. Ecker, The opposing effects of n-3 and n-6 fatty acids, Prog. Lipid Res. 47 (2008) 147–155. doi:10.1016/j.plipres.2007.12.004.

[6] M.I. Aveldano, A novel group of very long chain polyenoic fatty acids in dipolyunsaturated phosphatidylcholines from vertebrate retina, J. Biol. Chem. 262 (1987) 1172–1179.

[7] A. Poulos, Very long chain fatty acids in higher animals—A review, Lipids. 30 (1995) 1–14. doi:10.1007/BF02537036.

[8] M.-P. Agbaga, M.N. a Mandal, R.E. Anderson, Retinal very long-chain PUFAs:

new insights from studies on ELOVL4 protein., J. Lipid Res. 51 (2010) 1624–42. doi:10.1194/jlr.R005025.

[9] P. Barabas, A. Liu, W. Xing, C.-K. Chen, Z. Tong, C.B. Watt, B.W. Jones, P.S. Bernstein, D. Križaj, Role of ELOVL4 and very long-chain polyunsaturated fatty acids in mouse models of Stargardt type 3 retinal degeneration., Proc. Natl. Acad. Sci. U. S. A. 110 (2013) 5181–6. doi:10.1073/pnas.1214707110.

[10] R. Harkewicz, H. Du, Z. Tong, H. Alkuraya, M. Bedell, W. Sun, X. Wang, Y.H. Hsu, J. Esteve-Rudd, G. Hughes, Z. Su, M. Zhang, V.S. Lopes, R.S. Molday, D.S. Williams, E. a. Dennis, K. Zhang, Essential role of ELOVL4 protein in very long chain fatty acid synthesis and retinal function, J. Biol. Chem. 287 (2012) 11469–11480. doi:10.1074/jbc.M111.256073.

[11] A. Liu, R. Terry, Y. Lin, K. Nelson, P.S. Bernstein, Comprehensive and sensitive quantification of long-chain and very long-chain polyunsaturated fatty acids in small samples of human and mouse retina., J. Chromatogr. A. 1307 (2013) 191–200. doi:10.1016/j.chroma.2013.07.103.

[12] O. Berdeaux, P. Juaneda, L. Martine, S. Cabaret, L. Bretillon, N. Acar, Identification and quantification of phosphatidylcholines containing very-long-chain polyunsaturated fatty acid in bovine and human retina using liquid chromatography/tandem mass spectrometry., J. Chromatogr. A. 1217 (2010) 7738–48. doi:10.1016/j.chroma.2010.10.039.

[13] R. Taguchi, M. Ishikawa, Precise and global identification of phospholipid molecular species by an Orbitrap mass spectrometer and automated search engine Lipid Search, J. Chromatogr. A. 1217 (2010) 4229–4239. doi:10.1016/j.chroma.2010.04.034.

[14] X. Li, A.A. Franke, Improved LC-MS Method for the Determination of Fatty

Acids in Red Blood Cells by LC-Orbitrap MS, (2011) 3192–3198.

[15] L. Tedone, R. Costa, S. De Grazia, S. Ragusa, L. Mondello, Monodimensional (GC-FID and GC-MS) and comprehensive two-dimensional gas chromatography for the assessment of volatiles and fatty acids from ruta chalepensis aerial parts, Phytochem. Anal. 25 (2014) 468–475. doi:10.1002/pca.2518.

[16] M. Volpato, J.A. Spencer, A.D. Race, A. Munarini, A. Belluzzi, A.J. Cockbain, M.A. Hull, P.M. Loadman, A liquid chromatography–tandem mass spectrometry method to measure fatty acids in biological samples, J. Chromatogr. B. 1055–1056 (2017) 125–134. doi:10.1016/j.jchromb.2017.04.030.

[17] J. Pettersen, Determination of trans double bonds in polyunsaturated fatty acid methyl esters from their electron impact mass spectra Research Paper, 105 (2003) 156–164.

[18] D.-P. Kloos, E. Gay, H. Lingeman, F. Bracher, C. Müller, O. a Mayboroda, A.M. Deelder, W.M. a Niessen, M. Giera, Comprehensive gas chromatography-electron ionisation mass spectrometric analysis of fatty acids and sterols using sequential one-pot silylation: quantification and isotopologue analysis., Rapid Commun. Mass Spectrom. 28 (2014) 1507–14. doi:10.1002/rcm.6923.

[19] T. Portolés, L. Cherta, J. Beltran, F. Hernández, Improved gas chromatography-tandem mass spectrometry determination of pesticide residues making use of atmospheric pressure chemical ionization, J. Chromatogr. A. 1260 (2012) 183–192. doi:10.1016/j.chroma.2012.08.009.

[20] M. Raro, T. Portolés, J. V Sancho, E. Pitarch, F. Hernández, J. Marcos, R. Ventura, C. Gómez, J. Segura, O.J. Pozo, Mass spectrometric behavior of anabolic androgenic steroids using gas chromatography coupled to atmospheric pressure chemical ionization source. Part I: ionization., J. Mass Spectrom. 49

(2014) 509–21. doi:10.1002/jms.3367.

[21] E. Hurtado-Fernández, T. Pacchiarotta, E. Longueira-Suárez, O. a Mayboroda, A. Fernández-Gutiérrez, A. Carrasco-Pancorbo, Evaluation of gas chromatography-atmospheric pressure chemical ionization-mass spectrometry as an alternative to gas chromatography-electron ionization-mass spectrometry: avocado fruit as example., J. Chromatogr. A. 1313 (2013) 228–44. doi:10.1016/j.chroma.2013.08.084.

[22] R. García-Villalba, T. Pacchiarotta, A. Carrasco-Pancorbo, A. Segura-Carretero, A. Fernández-Gutiérrez, A.M. Deelder, O.A. Mayboroda, Gas chromatography-atmospheric pressure chemical ionization-time of flight mass spectrometry for profiling of phenolic compounds in extra virgin olive oil, J. Chromatogr. A. 1218 (2011) 959–971. doi:10.1016/j.chroma.2010.12.014.

[23] K. Hennig, J.P. Antignac, E. Bichon, M.-L. Morvan, I. Miran, S. Delaloge, J. Feunteun, B. Le Bizec, Steroid hormone profiling in human breast adipose tissue using semi-automated purification and highly sensitive determination of estrogens by GC-APCI-MS/MS, Anal. Bioanal. Chem. 410 (2018) 259–275. doi:10.1007/s00216-017-0717-8.

[24] E. Bichon, I. Guiffard, A. Vénisseau, E. Lesquin, V. Vaccher, A. Brosseaud, P. Marchand, B. Le Bizec, Simultaneous determination of 16 brominated flame retardants in food and feed of animal origin by fast gas chromatography coupled to tandem mass spectrometry using atmospheric pressure chemical ionisation, J. Chromatogr. A. 1459 (2016) 120–128. doi:10.1016/j.chroma.2016.07.003.

[25] F. Hernández, M. Ibáñez, T. Portolés, M.I. Cervera, J. V Sancho, F.J. López, Advancing towards universal screening for organic pollutants in waters., J. Hazard. Mater. 282 (2015) 86–95. doi:10.1016/j.jhazmat.2014.08.006.

[26] L. Cherta, T. Portolés, J. Beltran, E. Pitarch, J.G.J. Mol, F. Hernández, Application of gas chromatography-(triple quadrupole) mass spectrometry with atmospheric pressure chemical ionization for the determination of multiclass pesticides in fruits and vegetables, J. Chromatogr. A. 1314 (2013) 224–240. doi:10.1016/j.chroma.2013.09.029.

[27] M.I. Aveldano, H. Sprecher, Very long chain (C24 to C36) polyenoic fatty acids of the n-3 and n-6 series in dipolyunsaturated phosphatidylcholines from bovine retina., J. Biol. Chem. 262 (1987) 1180–1186.

[28] A. Liu, Y. Lin, R. Terry, K. Nelson, P.S. Bernstein, Role of long-chain and very-long-chain polyunsaturated fatty acids in macular degenerations and dystrophies, Clin. Lipidol. 6 (2011) 593–613. doi:10.2217/clp.11.41.

[29] A. Liu, J. Chang, Y. Lin, Z. Shen, P.S. Bernstein, Long-chain and very long-chain polyunsaturated fatty acids in ocular aging and age-related macular degeneration., J. Lipid Res. 51 (2010) 3217–29. doi:10.1194/jlr.M007518.

[30] D.R. Tocher, Omega-3 long-chain polyunsaturated fatty acids and aquaculture in perspective, Aquaculture. 449 (2015) 94–107. doi:10.1016/j.aquaculture.2015.01.010.

[31] S. Li, Ó. Monroig, T. Wang, Y. Yuan, J. Carlos Navarro, F. Hontoria, K. Liao, D.R. Tocher, K. Mai, W. Xu, Q. Ai, Functional characterization and differential nutritional regulation of putative Elovl5 and Elovl4 elongases in large yellow croaker (Larimichthys crocea), Sci. Rep. 7 (2017). doi:10.1038/s41598-017-02646-8.

[32] G. Carmona-Antoñanzas, Ó. Monroig, J.R. Dick, A. Davie, D.R. Tocher, Biosynthesis of very long-chain fatty acids (C>24) in Atlantic salmon: Cloning, functional characterisation, and tissue distribution of an Elovl4

elongase, Comp. Biochem. Physiol. - B Biochem. Mol. Biol. 159 (2011) 122–129. doi:10.1016/j.cbpb.2011.02.007.

[33] A. Jakobsson, R. Westerberg, A. Jacobsson, Fatty acid elongases in mammals: Their regulation and roles in metabolism, Prog. Lipid Res. 45 (2006) 237–249. doi:10.1016/j.plipres.2006.01.004.

[34] Folch J.; Lees M.; Stanley G. H. S., J. Folch, M. Lees, G.H.S. Stanley, A simple method for the isolation and purification of total lipids from animal tissues, J Biol Chem. 226 (1957) 497–509. doi:10.1007/s10858-011-9570-9.

[35] R.E. Olsen, R.J. Henderson, The rapid analysis of neutral and polar marine lipids using double-development HPTLC and scanning densitometry, J. Exp. Mar. Bio. Ecol. 129 (1989) 189–197. doi:10.1016/0022-0981(89)90056-7.

[36] J.C. Navarro, F. Amat, J.R. Sargent, A study of the variations in lipid levels, lipid class composition and fatty acid composition in the first stages of Artemia sp., Mar. Biol. 111 (1991) 461–465. doi:10.1007/BF01319419.

[37] W.W. Christie, Lipid analysis, Pergamon Press Oxford; 2nd edition, 1982.

[38] T. Portolés, C. Sales, B. Gómara, J.V. Sancho, J. Beltrán, L. Herrero, M.J. González, F. Hernández, Novel analytical approach for brominated flame retardants based on the use of gas chromatography-atmospheric pressure chemical ionization-tandem mass spectrometry with emphasis in highly brominated congeners., Anal. Chem. 87 (2015) 9892–9. doi:10.1021/acs.analchem.5b02378.

Table 1. List of PUFAs identified in the fish eye samples analyzed from the different species

Compounds	European seabass	Gilthead seabream	Senegalese sole	Atlantic salmon
20:4ω6	✓	✓	✓	✓
20:5ω3	✓	✓	✓	✓
22:6ω3	✓	✓	✓	✓
22: 5ω6	✓	✓	✓	✓
22:5ω3	✓	✓	✓	✓
24:6ω3	✓	✓	✓	✓
26:6ω3	✓	✓		
28:6ω3	✓	✓		
30:6ω3	✓	✓	✓	
32:6ω3	✓	✓	✓	✓
34:6ω3	✓	✓		

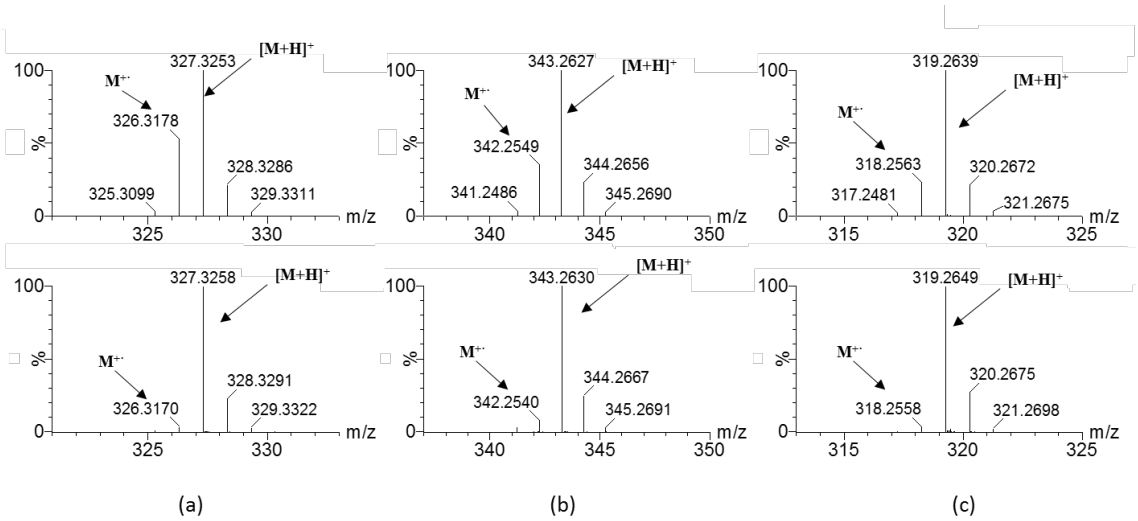
100
%
0
327.3253
[M+H]+
M+·
326.3178
328.3286
325.3099
329.3311
325
330
m/z
343.2627
[M+H]+
M+·
342.2549
344.2656
341.2486
345.2690
340
345
350
319.2639
[M+H]+
M+·
318.2563
320.2672
317.2481
321.2675
315
320
325
327.3258
[M+H]+
M+·
328.3291
326.3170
329.3322
343.2630
[M+H]+
M+·
344.2667
342.2540
345.2691
319.2649
[M+H]+
M+·
320.2675
318.2558
321.2698

(a) (b) (c)

Figure 1

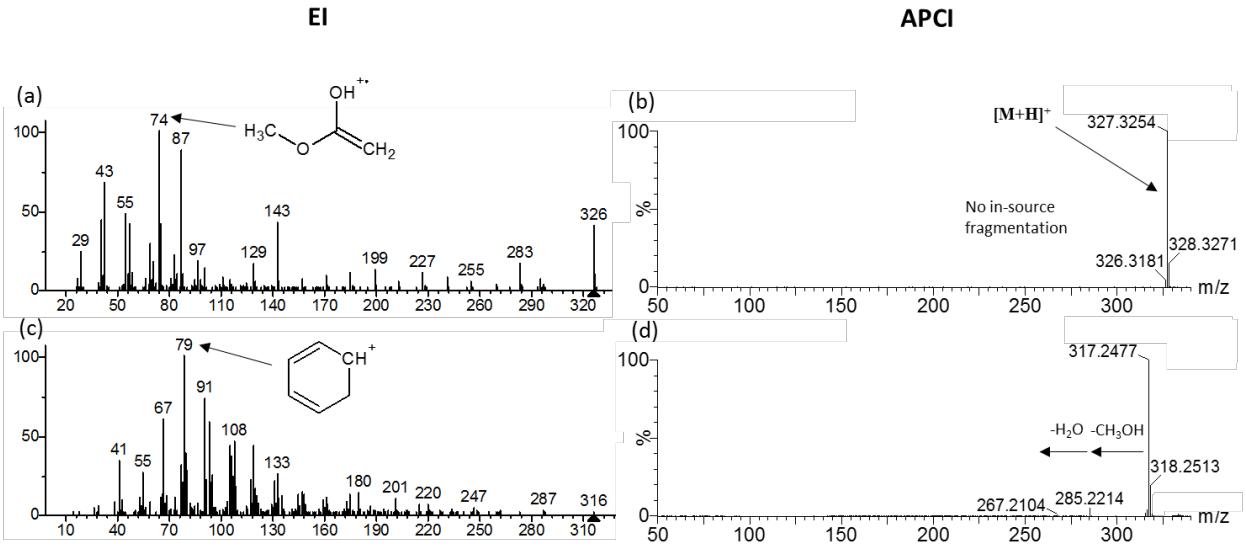
EI
APCI
(a)
(b)
(c)
(d)
[M+H]+
327.3254
No in-source
fragmentation
328.3271
326.3181
m/z
317.2477
-H2O -CH3OH
318.2513
267.2104
285.2214

Figure 2

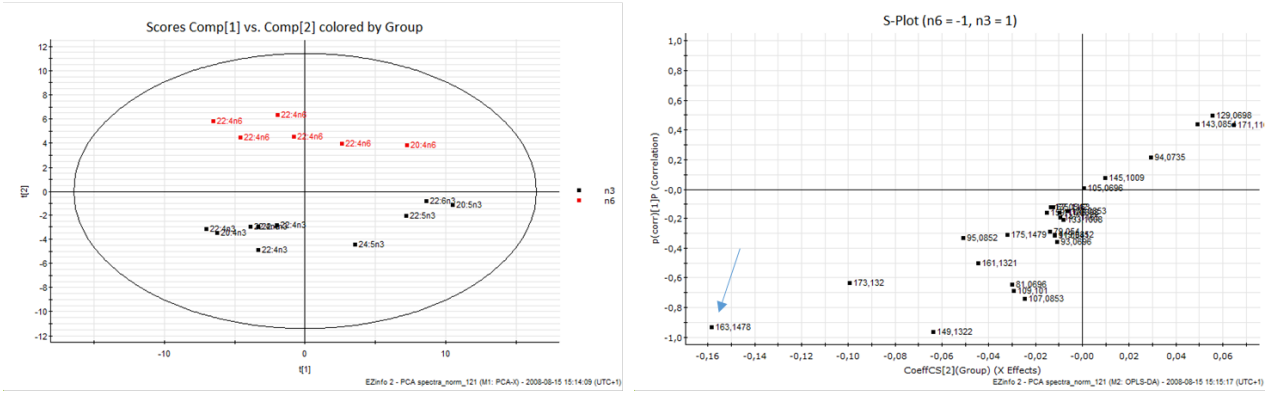
Scores Comp[1] vs. Comp[2] colored by Group
t[2]
t[1]
n3
n6
22:4n6
20:4n6
22:6n3
20:5n3
22:5n3
24:5n3
22:4n3
EZinfo 2 - PCA spectra_norm_121 (M1: PCA-X) - 2008-08-15 15:14:09 (UTC+1)
S-Plot (n6 = -1, n3 = 1)
p(corr)[1]P (Correlation)
CoeffCS[2](Group) (X Effects)
129,0698
94,0735
145,1009
105,0696
95,0852
175,1479
161,1321
173,132
107,0853
163,1478
149,1322
EZinfo 2 - PCA spectra_norm_121 (M2: OPLS-DA) - 2008-08-15 15:15:17 (UTC+1)

(a) (b)

Figure 3

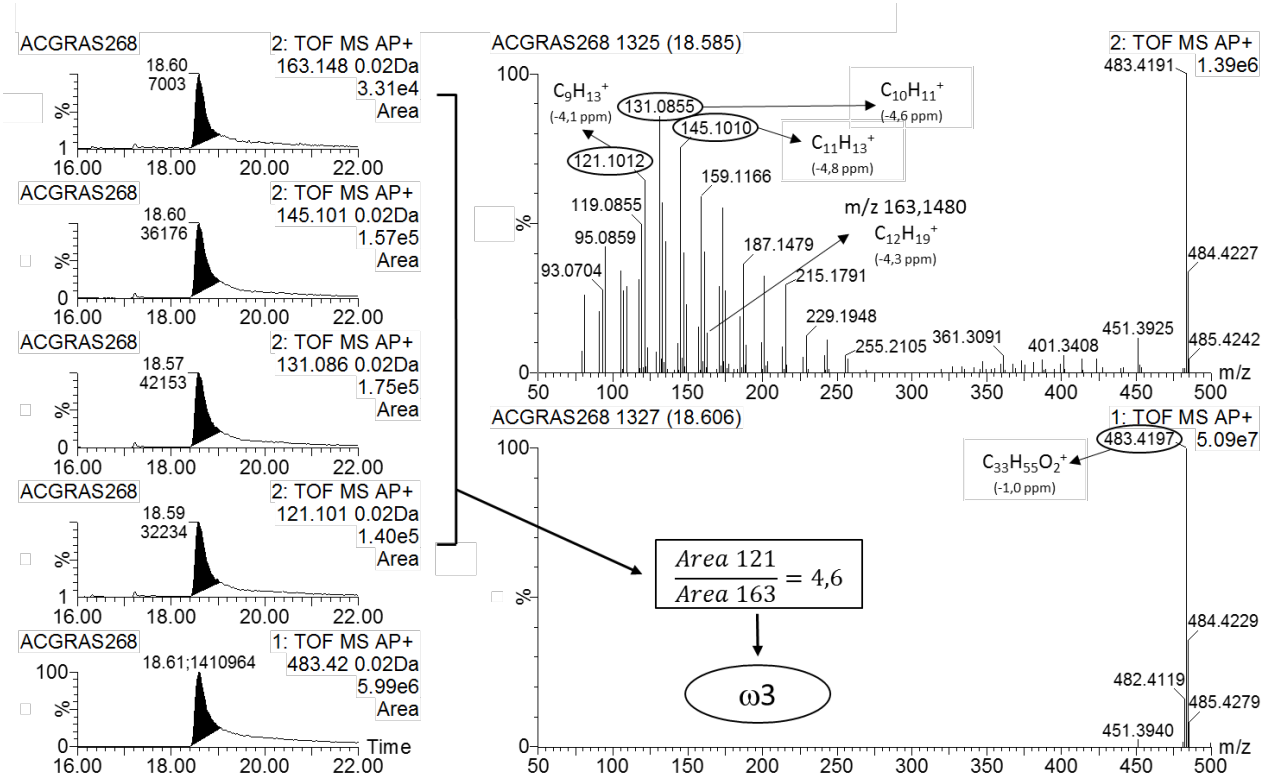
ACGRAS268
2: TOF MS AP+
163.148 0.02Da
3.31e4
Area
18.60
7003
ACGRAS268
2: TOF MS AP+
145.101 0.02Da
1.57e5
Area
18.60
36176
ACGRAS268
2: TOF MS AP+
131.086 0.02Da
1.75e5
Area
18.57
42153
ACGRAS268
2: TOF MS AP+
121.101 0.02Da
1.40e5
Area
18.59
32234
ACGRAS268
1: TOF MS AP+
483.42 0.02Da
5.99e6
Area
18.61;1410964
Time
ACGRAS268 1325 (18.585)
2: TOF MS AP+
1.39e6
483.4191
C9H13+ (-4,1 ppm)
131.0855
C10H11+ (-4,6 ppm)
145.1010
C11H13+ (-4,8 ppm)
121.1012
159.1166
119.0855
95.0859
93.0704
187.1479
215.1791
m/z 163,1480
C12H19+ (-4,3 ppm)
229.1948
255.2105
361.3091
401.3408
451.3925
484.4227
485.4242
m/z
ACGRAS268 1327 (18.606)
1: TOF MS AP+
5.09e7
483.4197
C33H55O2+ (-1,0 ppm)
Area 121 / Area 163 = 4,6
ω3
484.4229
482.4119
485.4279
451.3940
m/z
(a)
(b)

Figure 4

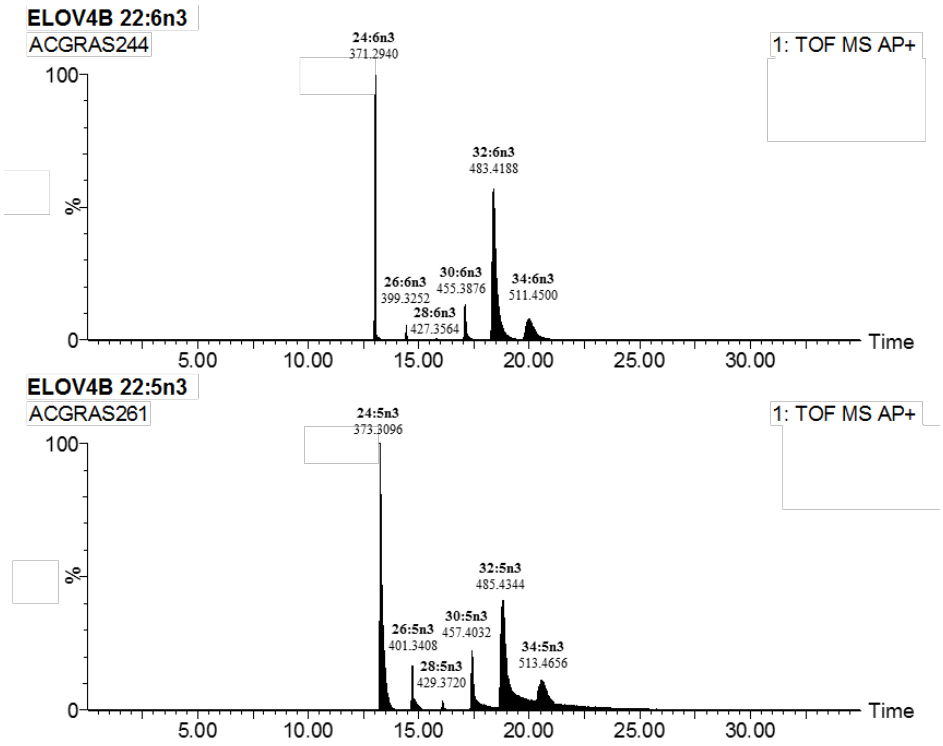
ELOV4B 22:6n3
ACGRAS244
1: TOF MS AP+
24:6n3
371.2940
32:6n3
483.4188
26:6n3
399.3252
30:6n3
455.3876
34:6n3
511.4500
28:6n3
427.3564
100
%
0
5.00
10.00
15.00
20.00
25.00
30.00
Time
ELOV4B 22:5n3
ACGRAS261
1: TOF MS AP+
24:5n3
373.3096
32:5n3
485.4344
26:5n3
401.3408
30:5n3
457.4032
34:5n3
513.4656
28:5n3
429.3720
100
%
0
5.00
10.00
15.00
20.00
25.00
30.00
Time

Figure 5